Propagation and self-healing properties of Lommel-Gaussian beam through atmospheric turbulence*

CHEN Xiang (陈祥)[1], **YUAN Yabo** (袁亚博)[2], **YAN Baoluo** (闫宝罗)[3], **ZHANG Ruoyu** (张若禹)[2], **LIU Haifeng** (刘海锋)[3,4]**, **LU Zehui** (陆泽辉)[3], **and LIU Bo** (刘波)[3,4]

1. China Academy of Space Technology, Xi'an 710100, China

2. Beijing Institute of Tracking and Telecommunication Technology, Beijing 100094, China

3. Tianjin Key Laboratory of Optoelectronic Sensor and Sensing Network Technology, Institute of Modern Optics, Nankai University, Tianjin 300350, China

4. Southern Marine Science and Engineering Guangdong Laboratory, Zhuhai 519000, China

(Received 18 January 2021; Revised 29 January 2021)

The superposition of basic non-diffracting beams triggered new research hotspots lately, laying opportunities for long-distance wireless optical communication. The Lommel-Gaussian (LMG) beam formed by the superposition of Bessel-Gaussian light not only possesses non-diffraction feature, but also has tunable symmetry. With the help of Poynting vector analysis, we observed a smaller radial energy flow component during the propagation of the high order symmetrical LMG beam, which allows it to maintain the original beam profile over long distance. Thanks to the energy oscillation of the mainlobe and sidelobes, the mainlobe blocked by the symmetrical LMG beam can be restored. Also, the random phase screen with angular spectrum method is used to describe the beam behaviors in turbulence. The results show that the symmetry LMG is preferred in free space optical communication, and the asymmetric LMG performs poorly due to asymmetric energy transfer.

Document code: A **Article ID:** 1673-1905(2021)09-0572-5

DOI https://doi.org/10.1007/s11801-021-1007-4

Recently, a series of special beams have attracted widespread attention in the field of turbulence suppression. Taking advantage of their diffraction-free and stable wavefronts properties, long-distance transmission with smaller divergence can be achieved. Compared with traditional turbulence suppression schemes (e.g., adaptive optics, radio frequency/free space optics hybrid systems, multiple-input multiple-output[1]), using special beam has an absolute advantage in the case of system simplicity, which can be prepared only by designing a phase hologram or phase plate reasonably[2].

As a typical case, Weng et al[3] realized the ultralong anti-diffracting beam based on the principle of multiple energy oscillation in 2018, which clearly explains the mechanism of non-diffracting beams for long-distance propagation. Zhang et al[2] prepared a shape-preserving optical pin beams (OPB) in 2019 and achieved excellent turbulence suppression results, based on the principle of transverse wave vector elimination. Actually, the OPB is a superposition of radially symmetric Airy beams. It can be concluded that the combination of the above beams will open up new prospects for optical communication. Some other “diffraction-free” beams, such as Bessel beams[3], Mathieu beams[4] and Airy beam[3] have been extensively studied and reported. Their self-healing and self-accelerating properties are also very suitable for optical communication or optical interconnection.

Similarly, Kovalev et al[5], proposed a symmetrically tunable quasi-non-diffracting beam in 2014, called Lommel beam, which is the linear superposition of Bessel modes with identical axial projection of the wave vector. As a member of non-diffracting beam family, ideal Lommel beams with infinite energy is physically unrealizable. Therefore, only Lommel-Gaussian (LMG) beam with finite energy and apertures can be achieved in experiments, which is similar to traditional Bessel-Gaussian (BG) beam[6]. The high-order LMG beam has a spiral phase distribution and presents a 'doughnut' shapes in intensity profile, so it can be used to carry orbital angular momentum (OAM) for space division multiplexing like traditional Laguerre-Gaussian (LG) beam. Besides, with continuously tunable symmetry and OAM,

* This work has been supported by the National Key R&D Program of China (No.2018YFB1802302), the National Natural Science Foundation of China (Nos.11774181, 61727815, 11274182, 11904180, 11804250 and 1190426), the Natural Science Foundation of Tianjin (Nos.19JCYBJC16700 and 20JCQNJC01480), the Science and Technology Project of Tianjin (No.20YDTPJC00760), and the Tianjin Development Program for Innovation and Entrepreneurship.

** E-mail: hfliu@nankai.edu.cn

LMG beams exhibit excellent potential applications in some basic research fields such as optical tweezers, microscopic imaging. In 2015, Zhao et al[7] reported the first generation of various LMG beams using digital micromirror devices (DMD), leading the above vision possible.

In terms of optical communication, Yu et al[8] calculated the propagation feature of a symmetrical LMG in non-Kolmogorov turbulence based on the spiral harmonic expansion method in 2017. In the same year, they continued to theoretically study the crosstalk properties of symmetrical LMG beams in ocean turbulence[9]. Until 2020, our previous work reported the application of LMG beams in optical communication for the first time, and discussed the influence of symmetry on OAM channel crosstalk carried by LMG beams both theoretically and experimentally. Also, we demonstrated the multiplexed superposition state generation method of asymmetric LMG beams[10,11].

In this letters, we tend to clearly explain physical reason for the enhanced anti-turbulence ability of LMG beam over LG beams, and dicuss the field and energy flow evolution during propagation using the theory of diffraction's anglar spectrum transfer and random phase screen methods.

The field distribution under cylindrical coordinates can be written as[10]

$$\mathrm{LMG}_l(r,\varphi,z)=q^{-1}(z)\exp[\mathrm{i}kz-\mathrm{i}zk_r^2/2kq(z)-r^2/\omega_0^2q(z)]\times\sum_{p=0}^{\infty}(-c^{2p})\exp[\mathrm{i}(l+2p)\varphi]\times J_{l+2p}[k_r r/q(z)], \quad (1)$$

where r, φ, z are the radial position, azimuthal angle and propagation distance in cylindrical coordinates, respectively. $k=2\pi/\lambda$ is wavenumber with wavelength λ, $k_r=\beta k$ is transverse wave vector with scaling factor β, l is the topological charge, and p is the radial mode numbers. ω_0 denotes initial radius of Gaussian envelop, $q(z)$ is defined as $q(z)=1+\mathrm{i}2z/(k\omega_0^2)$, and $J_{l+2p}(\cdot)$ is Bessel function of the first kind. Importantly, c is the asymmetry factor, whose modulus can tune the asymmetry of transverse intensity and is limited in $|c|<1$. Its phase angle defines the rotation angle of the LMG beam.

As shown in Fig.1(a-d), by tuning the phase angle of c, the transverse distribution can be symmetrical around any angle. From Fig.1(d-f), one can clearly see that the absolute value of c can adjust the circular symmetry of the transverse field. As $|c|$ increases, the asymmetry of LMG mode would gradually increase. Moreover, scaling factor β can control the size of the transverse field in Figs.1(d), (g) and (h), which is similar to the p of LG beam[12]. According to its electromagnetic field expression Eq.(1), we can design phase holograms to load into the spatial light modulator to generate the corresponding beams.

We calculated the propagation properties of the LMG beam using angular spectrum diffraction theory, which offers a more reliable application range[13]. $U_0(x_0, y_0)$ and $U(x, y)$ are the initial field and diffraction field at Δz plane, respectively, which can be written as

$$U(m\Delta x,n\Delta y)=\mathrm{IFFT}\{\mathrm{FFT}[U_0(m'\Delta x_0,n'\Delta y_0)]\times\exp[\mathrm{i}k\Delta z\sqrt{1-(\lambda p\Delta f_x)^2-(\lambda q\Delta f_y)^2}]\}, \quad (2)$$

where FFT and IFFT denote fast Fourier transform and inverse Fourier transform, respectively. In order to adapt to the random phase screen method in simulating turbulence effect section, we adopted the following configuration. The size and pixels of simulating region/ phase screen are $\Delta L\times\Delta L$ and $N\times N$, respectively. So the spatial sampling interval and spatial frequency sampling interval are $\Delta x=\Delta y=\Delta L/N$ and $\Delta f_x=\Delta f_y=1/\Delta L$, respectively. $m'=n'=-N/2, -N/2+1, \ldots, N/2-1$ is the discretization process. The simulation parameters in Tab.1 are assumed unless ortherwise specified. Besides, as shown in Tab.1, the waist width setting for LG and LMG beams are different, owing to the scaling factor β of LMG beams. We need to set the waist width of the LMG beams to be slightly larger to ensure that the mainlobe sizes of two beams are equal on the initial plane.

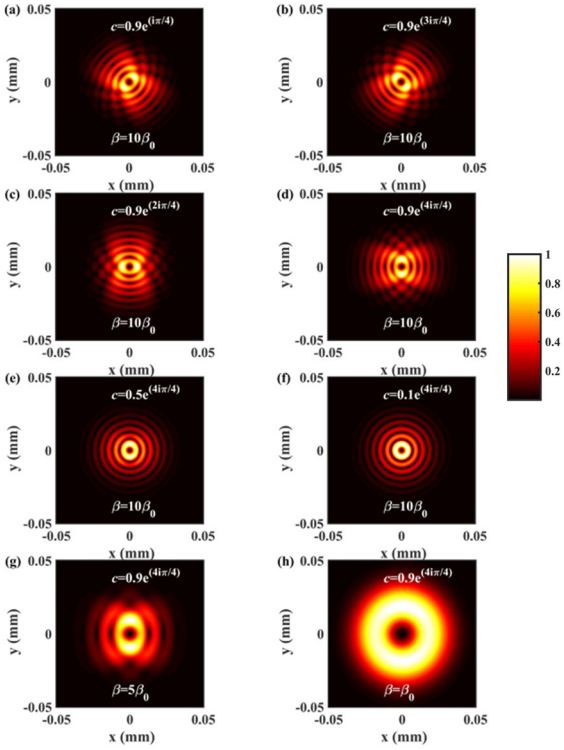

Fig.1 The transverse field distribution of LMG with basic parameters of $\beta_0=1.67\times10^{-4}$, $\omega_0=0.02$ m, $l=2$ and different asymmetry factor c or scaling factor β

In order to clearly illustrate the divergence of the light energy, we use the fellowing normalized intensity formula:

$$I(z)=\frac{|\int_0^{\omega_0}\int_0^{2\pi}U(r,\varphi,z)\mathrm{d}r\mathrm{d}\varphi|^2}{\max_{0\to z_{\mathrm{total}}}\{|\int_0^{\omega_0}\int_0^{2\pi}U(r,\varphi,z)\mathrm{d}r\mathrm{d}\varphi|^2\}}. \quad (3)$$

Note that, the radial area in Eq.(3) should be limited to the initial waist width ω_0 . As shown in Fig.2(a) and (c), unlike the gradual divergence of the $\mathrm{LG}_{l=0}$ beam with the

propagation distance, the symmetrical LMG $_{l=0,|c|=0.1}$ beam shows a long self-focusing distance (over 60 m under current beam parameters), which is similar to the OPB beam behaviors[2]. Based on the above phenomena, we expect that LMG beams possess self-healing or self-reconstruction properties like BG beams. According to the Weng's theory[6], non-diffracting effect is based on transverse energy transfer between central maximum and peripheral rings. Hence, a circular obstacle with a radius of r' (see Tab.1) is placed at the center of the source plane to block the mainlobe of beams. From the diffraction pattern in Fig.2(b) and (d), one can clearly see that the blocked central energy re-appears after being propagating tens of meters. However, owing to the natural divergence of the LG beam as mentioned above, the energy divergence in the center is very serious, while the symmetrical LMG beam can maintain the reconstructed center energy at a long distance. In addition, the energy transition of the LMG beam during the reconstruction process is more stable than that of the LG beam, according to the normalized intensity curve.

Tab.1 Parameters used in numerical calculation

Parameter	Symbol	Value
Wavelength	λ	1 550 nm
Propagation distance	z_{total}	150 m
Thickness of turbulent layer	Δz	1 m
Phase screen size	$\Delta L\times\Delta L$	0.5 m×0.5 m
Phase screen pixels	$N\times N$	1 000×1 000
Non-Kolmogorov turbulence-parameter	a	11/3
Waist width of LG in initial plane (*)	ω_0	0.02 m
Waist width of LMG in initial plane (*)	ω_0	0.01 m
Scaling factor of LMG	β	1.67×10^{-4}
Obstruction size at mainlobe	r'	0.005 m
Obstruction size at sidelobe	r''	0.01 m
Obstruction offset at sidelobe	r'''	0.01 m

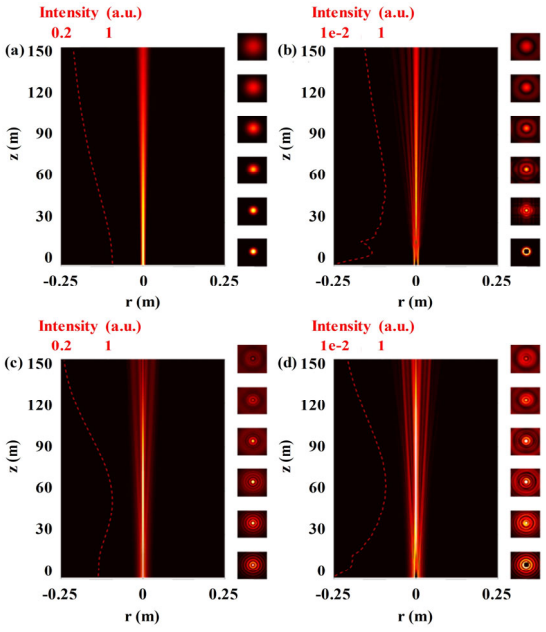

Fig.2 Propagation properties of LG$_{l=0}$ beam in (a) free space and (b) blocked by circular obstacle at source plane; (c) LMG $_{l=0,|c|=0.1}$ in free space condition; (d) LMG $_{l=0,|c|=0.1}$ under blocked condition (The insets give the transverse field at each ordinate scale value, and the red dotted line is the normalized intensity evolution of the beam mainlobe.)

In order to clearly illustrate the physical process of the self-reconstruction of the LMG beam, we calculated the Poynting vector / energy flow vector after destruction, which is given by[3]

$$\boldsymbol{s}=\boldsymbol{s}_z+\boldsymbol{s}_\perp=(1/2\eta_0)|U|^2\boldsymbol{z}+(i/4\eta_0 k)(U\nabla_\perp U^*-U^*\nabla_\perp U), \quad (4)$$

where $\boldsymbol{s}_\perp$ and $\boldsymbol{s}_z$ are the the longitudinal and transverse components of the Poynting vector, respectively. $\eta_0=\sqrt{\mu_0/\varepsilon_0}$ indicates the free space impedence.

In the first part of the propagation (~30 m), the energy of the sidelobes is transferred to the blocked central area, which corresponds to the process of beam self-focusing. When the LMG beam travels to around 63 m, the inward and outward energy flow balances, a sufficiently strong field in the center can be seen. At 90 m of propagation, the energy flow of the mainlobe and sidelobes are directed from the inside to the outside, which means that the beam is experiencing divergence.

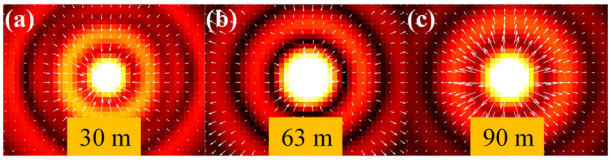

Fig.3 Calculated transverse power flow $\boldsymbol{s}_\perp$ of LMG $_{l=0,|c|=0.1}$ beam with blocked mainlobe propagating at (a) 30 m, (b) 63 m and (c) 90 m, respectively

For high-order fields (i.e., vortex light state), our focus is the reconstruction process of the sidelobes. A circular obstacle with a radius of r'' is built on the initial plane with r''' offsets (see Tab.1), which destroys both the sidelobes and the mainlobe of LMG beams. As shown in Fig.4, owing to the vortex phase, both beams can recover most of the blocked parts during propagation. Importantly, the symmetrical LMG beam can almost maintain its original beam size, while LG beam exhibits a larger divergence. The former is preferred by free optical communication. However, the asymmetric LMG$_{l=3,|c|=0.9}$ beam does not perform well. Although the central light field is reconstructed, most of the energy is dispersed to the sidelobes, which means that the asymmetric LMG beam may not be suitable for applications in turbulent environments. The above explains the result of high crosstalk occurred in the asymmetric LMG beam in our previous work from the perspective of the field[10]. Also, some works indicated that the asymmetric energy transfer may cause serious degradation in one direction in turbulence[14].

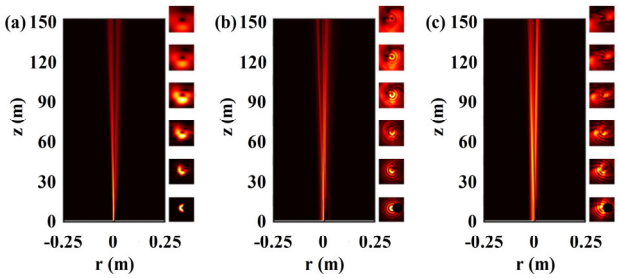

Fig.4 Propagation properties of (a) LG$_{l=3}$, (b) LMG$_{l=3,|c|=0.1}$, (c) LMG $_{l=3,|c|=0.9}$ beam with blocked sidelobes

The results of energy flow analysis indicate that the sidelobes of the 'doughnut-shaped' high-order beams can be well restored during the propagation. By carefully observing the energy flow of the LG beam (Fig.5(a1-a4)) and the symmetrical LMG beam (Fig.5(b1-b4)) in various propagation planes, one can find that the symmetrical LMG beam has a smaller radial component of energy flow, which leads to the LMG can maintain its size in a long distance.

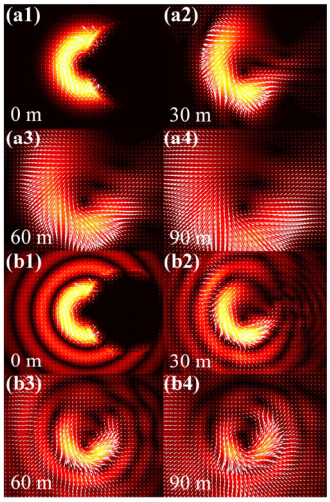

Fig.5 Calculated transverse power flow $s_{\perp}$ of (a1-a4) LG$_{l=3}$ and (b1-b4) LMG$_{l=3,|c|=0.1}$ beam with blocked sidelobes propagating at 0 m, 30 m, 60 m and 90 m

Using the random phase screen method and diffraction theory, we simulated the propagation behavior of the above two types of beams under different turbulence intensities. The non-Kolmogorov spectrum of turbulent atmosphere in this simulation is represented by[15]

$$\Phi_{\text{atm}}(\alpha,\kappa)=\frac{\Gamma(\alpha-1)\cos(\alpha\pi/2)C_n^2\kappa^{-\alpha}}{4\pi^2},\quad (3<\alpha<5), \quad (5)$$

where Γ is the Gamma function, α is the power-law exponent of the non-Kolmogorov spectrum, C_n^2 is the the refractive index structure parameter, and κ is spatial frequency. So the phase modulation on the slice can be written as

$$\Phi_s(\kappa_x,\kappa_y)=2\pi k^2\Delta z\Phi_{\text{atm}}(\kappa_x,\kappa_y,\kappa_z=0). \quad (6)$$

Finally, the phase screen can be obtained through power spectrum inversion and low frequency compensation.

$$\phi_{\text{mask}}(m\Delta x,n\Delta y)=\frac{2\pi}{\Delta L}\text{IFFT}\{a(m',n')\Phi_s(m'\Delta f_x,n'\Delta f_y)^{1/2}\}. \quad (7)$$

The phase screen should match the previous angular spectrum calculation model. So m, n, m', n' in Eq.(7) should meet $m=n=m'=n'=-N/2, -N/2+1, \ldots, N/2-1$. $a=a+\mathbf{i}B$ is a complex Gaussian random matrix to filter the atmospheric turbulence power spectrum, in which A and B are both two dimensional Gaussian white noise with mean of 0 and variance of 1.

Parameters for simulation are shown in Tab.1, the demodulation results using phase conjugation method at each z are shown in Fig.6. As the strength of turbulence increases (i.e., C_n^2), all beams begin to deteriorate, such as multiple speckle formation, beam wandering. Nevertheless, the symmetrical LMG beams can still maintain a better profile compared to the other two. Asymmetrical LMG beams are even inferior to LG light under low-intensity turbulence (Fig.6(b1-b3)). Together with the results of self-reconstruction (Fig.4(c)), one can find that the orientation in the energy transfer process leads to possible beam walk-off. Additionally, the demodulated asymmetric LMG beam is not symmetrical, so it needs to be re-shaped to match the circularly symmetrical receiver. As far as we know, phase mask generated based on Gerchberg-Saxton algorithm is a fast convergence and implementable solution. While the symmetrical LMG beam can be demodulated under strong turbulence (Fig.6(b3)).

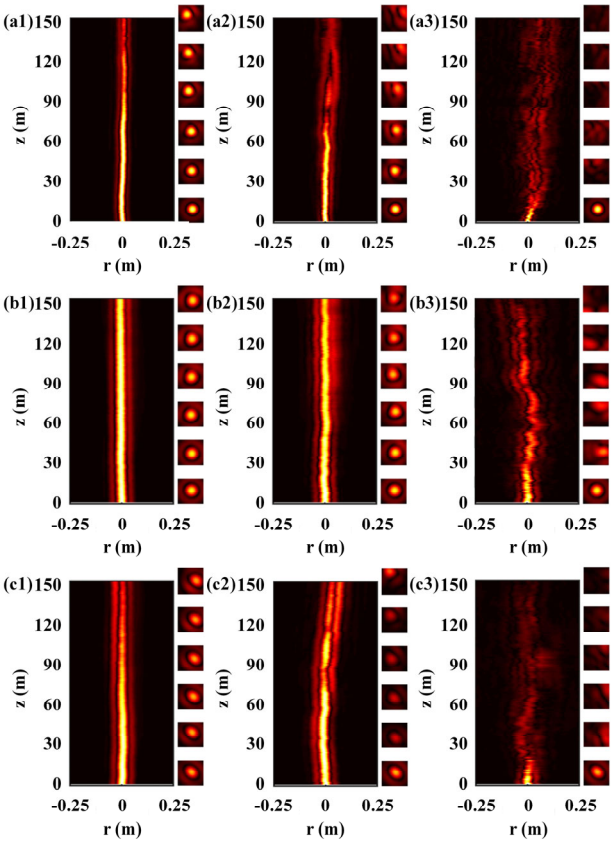

Fig.6 Simulated field distribution after demodulation over 150 m vs. different turbulence intensity by random phase screen methods: (a1) $LG_{l=3}^{demod.}$, $C_n^2=10^{-16}m^{3-\alpha}$; (a2) $LG_{l=3}^{demod.}$, $C_n^2=5\times10^{-16}m^{3-\alpha}$; (a3) $LG_{l=3}^{demod.}$, $C_n^2=5\times10^{-15}m^{3-\alpha}$; (b1) $LMG_{l=3,|c|=0.1}^{demod.}$, $C_n^2=10^{-16}m^{3-\alpha}$; (b2) $LMG_{l=3,|c|=0.1}^{demod.}$, $C_n^2=5\times10^{-16}m^{3-\alpha}$; (b3) $LMG_{l=3,|c|=0.1}^{demod.}$, $C_n^2=5\times10^{-15}m^{3-\alpha}$; (c1) $LMG_{l=3,c=0.9\exp(i3\pi/4)}^{demod.}$, $C_n^2=10^{-16}m^{3-\alpha}$; (c2) $LMG_{l=3,c=0.9\exp(i3\pi/4)}^{demod.}$, $C_n^2=5\times10^{-16}m^{3-\alpha}$; (c3) $LMG_{l=3,c=0.9\exp(i3\pi/4)}^{demod.}$, $C_n^2=5\times10^{-15}m^{3-\alpha}$

In conclusion, based on angular spectrum diffraction theory and random phase screen method, we perform beams propagation analysis to give a physical reason for the enhanced anti-turbulence ability of LMG beam over LG beams. For the blocked symmetrical LMG beam, most of the mainlobe energy can be recovered in the self-focusing range. Owing to the small radial energy flow component, the high-order LMG beam can better maintain its profile over LG beam. On the contrary, for asymmetric LMG beams, due to the asymmetry of the energy transfer during propagation, it exhibits greater sensitivity to turbulence. The beam wandering and multiple speckle still occur, despite the lower intensity turbulence. The simulation results presented in this work are expected to provide important reference for the design and optimization of novel beams for optical comunication.

References

[1] BaoluoYan, HaifengLiu, ChangjinLi, Xiaorui Jiang, Xiao-long Li, Jiaqing Hou, Hao Zhang, Wei Lin, Bo Liu and Jianguo Liu, Optics and Laser Technology **131**, 106391 (2020).

[2] Ze Zhang, Xinli Liang, Mihalis Goutsoulas, Denghui Li, Xiuting Yang, Shupeng Yin, Jingjun Xu, Demetrios N. Chris-todoulides, Nikolaos K. Efremidis and Zhigang Chen, APL Photonics **4**, 076103 (2019).

[3] Xiaoyu Weng, Qiang Song, Xiaoming Li, Xiumin Gao, Hanming Guo, Junle Qu and Songlin Zhuang, Nature Communications **9**, 5035 (2018).

[4] Chi-Young Hwang, Kyoung-Youm Kim and Byoungho Lee, Optics Express **19**, 7356 (2011).

[5] Peng Zhang, Yi Hu, Tongcang Li, Drake Cannan, Xiaobo Yin, Roberto Morandotti, Zhigang Chen and Xiang Zhang, Physical Review Letters **109**, 193901 (2012).

[6] V. V. Kotlyar, A. A. Kovalev and V. A. Soifer, Optics Letters **39**, 2395 (2014).

[7] Qian Zhao, Lei Gong and Yinmei Li, Applied Optics **54**, 7553 (2015).

[8] Lin Yu, Beibei Hu and Yixin Zhang, Optics Express **25**, 19538 (2017).

[9] Lin Yu and Yixin Zhang, Optics Express **25**, 22565 (2017).

[10] Baoluo Yan, Zehui Lu, Jinyao Hu, Tianxu Xu, Hao Zhang, Wei Lin, Yang Yue, Haifeng Liu and Bo Liu, IEEE Journal of Selected Topics in Quantum Electronics **27**, 7600310 (2021).

[11] Baoluo Yan, Zehui Lu, Jinyao Hu, Tianxu Xu, Hao Zhang, Wei Lin, Huanbao Wu, Haifeng Liu and Bo Liu, Orbital Angular Momentum (OAM) Carried by Asymmetric Vortex Beams for Wireless Communications: Theory, Experi-ment and Current Challenges, 14th Pacific Rim Conference on Lasers and Electro-Optics, Sydney, C4F_1 (2020).

[12] Long Li, Guodong Xie, Yan Yan, Yongxiong Ren, Peicheng Liao, Zhe Zhao, Nisar Ahmed, Zhe Wang, Changjing Bao, Asher J. Willner, Solyman Ashrafi, Moshe Tur and Alan E. Willner, Journal of the Optical Society of America B-Optical Physics **34**, 1 (2017).

[13] Junchang Li, Zujie Peng and Yunchang Fu, Optics Com-munications **280**, 243 (2007).

[14] Yahya Baykal, Optics Communications **393**, 29 (2017).

[15] Xueli Sheng, Yixin Zhang, Fengsheng Zhao, Licheng Zhang and Yun Zhu, Optics Letters **37**, 2607 (2012).